

## Experimental Study on the Behavior of Bounded Square Footing on Sandy Soil

Dr. Mohammed Y. Fattah 

Building and Construction Engineering Department, University of Technology/Baghdad

Dr. Kais T. Shlash

Building and Construction Engineering Department, University of Technology/ Baghdad

Husham A. Mohammed

Building and Construction Engineering Department, University of Technology/ Baghdad

Email:Sawsanakram@yahoo.com

Received on: 15/1/2013 & Accepted on: 4/7/2013

### ABSTRACT

Structural skirts are walls fixed to the edges of shallow foundations to improve their bearing capacities. Sometimes, the shallow foundation is bounded by a close obstruction like a wall. The presence of this wall has an effect on the bearing capacity of footing, whose behavior in this case can be similar to a skirted foundation in which a structural skirt is located at one side of the footing. The present study investigates the behavior of model footings bounded by a wall of different depths and located at different distances from the footing, resting on sandy soil. In this study, different parameters are considered such as relative density of sand (33 and 56) %, distance from wall to the edge of footing to width of footing ratio ( $h/B$ ) (zero, 0.5, 1, 1.5 and 2) and depth of wall to width of footing ratio ( $d/B$ ) (0.5, 1, 1.5 and 2).

Test results show that the presence of the wall affects remarkably the values of bearing capacity, leading to improvement in the values of bearing capacity with different percentages according to the distance from wall to the edge of footing to width of footing ratio ( $h/B$ ) and depth of wall to width of footing ratio ( $d/B$ ) due to the increase in soil confinement underneath the footing. In loose sand, the largest improvement in bearing capacity for square footing bounded by walls reaches (43) %, at ( $h/B = 0.5$ ) and ( $d/B = 2$ ). In medium sand, the largest improvement in bearing capacity for square footing bounded by walls reaches (56) %, at ( $h/B = 0.5$ ) and ( $d/B=2$ ). The bearing capacity increases with depth of the wall, the maximum effect of the wall on the bearing capacity is when the value of the depth of the wall ( $d/B$ ) is between (1.5-2.0), for square footing on sand of different densities.

**Keywords:** Square footing, bounded, wall, structural skirt, bearing capacity, sandy soil.

دراسة عملية عن تصرف الاساس المربع المحدد على تربة رملية

: الخلاصة

الحواف الإنشائية عبارة عن حواجز تثبت عند حافة الأسس الضحلة، لتحسين قيم قابلية تحملها. في بعض الأحيان، تحدد الأسس الضحلة بواسطة عارض مثل جدار. هذا الجدار يؤثر على قابلية التحمل للأساس، في هذه الحالة يمكن تشبيهه سلوك الأساس ب (الأسس المحددة بحواجز) في حالة كونها موضوعة عند جهة واحدة من الأساس. في هذه الدراسة، تم التعرف على تصرف موديل الأساس المربع المحدد بواسطة جدار والذي يوضع على أبعاد وأعماق مختلفة من الأسس المستندة على تربة رملية. تمت دراسة معاملات مختلفة مثل الكثافة النسبية للرمل (33 و 56) %، واستخدمت خمس مسافات بين الجدار والأساس ( $h/B$ ) هي (صفر، 0.5، 1، 1.5 و 2) وكذلك استخدمت أربعة أعماق للجدار ( $d/B$ ) هي (0.5، 1، 1.5 و 2). تظهر نتائج الفحوصات بأن وجود الجدار يؤثر بصورة كبيرة على قيم قابلية التحمل، حيث يؤدي الى تحسين في قيم قابلية التحمل بنسب مختلفة طبقاً إلى مسافة الجدار من حافة الأساس إلى عرض الأساس ( $h/B$ ) وعمق الجدار إلى عرض الأساس ( $d/B$ )، بسبب الزيادة في حصر التربة تحت الأساس. في الرمل المفكك، أكبر نسبة تحسين في قابلية التحمل للأساس (المربع) المحدد بواسطة الجدار تصل الى (43) % عند ( $h/B = 0.5$ ) و ( $d/B = 2$ ). أما في الرمل متوسط الكثافة، فإن أكبر نسبة تحسين لهذه الأسس المحددة بواسطة الجدار تصل إلى (56) % عند ( $h/B = 0.5$ ) و ( $d/B = 2$ ) بينما في الرمل الكثيف، أكبر نسبة تحسين في قابلية التحمل لنفس الأسس المحددة بواسطة الجدار تصل إلى (67) % عند ( $h/B = 0$ ) و ( $d/B = 2$ ). بينت النتائج كذلك أن قابلية التحمل تزداد مع زيادة عمق الجدار وأن أقصى تأثير لعمق الجدار ( $d/B$ ) على قابلية التحمل هو عندما يكون عمق الجدار بين (1.5 - 2) للأسس المربعة المستندة على الرمل بكثافات مختلفة.

## INTRODUCTION

Skirted foundation, in which vertical or inclined wall surrounds one or more sides of the soil mass beneath the footing, is one of the recognized bearing capacity improvement techniques as shown in Figure (1). Construction of vertical skirt at the base of the footing, confining the underlying soil, generates a soil resistance on skirt side that helps the footing to resist sliding (Saleh et al., 2008).

Skirted foundations fixed to the edges of shallow foundations have been used for a considerable time, principally to increase the "effective depth" of the foundations in marine and other situations where water scours may be a problem. This method of improvement does not need excavation of the soil, and hence it cannot be restricted by the presence of a high water table.

Sometimes, the shallow foundation is bounded by a close obstruction like wall. This wall has an effect on the bearing capacity of footing, whose behavior in this case can be similar to a skirted foundation in which a structural skirt is located at one side of the footing. The footing in this case is termed "bounded footing".

The objective of the present study is to determine the influence of the presence of wall at different distances and depths from the shallow foundation on the bearing capacity and settlement of sandy soils. The testing program consists of 42 model tests investigating parameters like distance of wall from the edge of footing, depth of the wall and relative density of sandy soil.

### Previous Studies (Related Literature)

**Rao and Narhari** (1979) developed a skirted plug foundation and indicated that the provision of skirting to the soil plug is generally beneficial and can be applied when the settlement is restricted for a given load.

**Rao and Ranjan** (1985) developed a method of computing settlement of foundations on weak subsoil deposits reinforced with granular piles. Full-scale in situ tests on skirted granular piles were carried out at four different sites consisting of loose/soft deposits. The settlement computations made by the proposed analytical

procedure were compared with observed values from field tests where a good correlation was noted.

**Byrne et al.** (2002) presented results from a laboratory investigation of the monotonic loading response of skirted shallow foundations on sand, with particular emphasis on loads relevant to the wind turbine problem. The investigation included varying the length of the skirt compared with the diameter of the foundation as well as varying the mineralogy and density of the sand deposits. Results from vertical bearing capacity tests were presented and compared with simple theoretical expressions based on standard bearing capacity formulae. Results from applied moment loading tests were also presented, from which it was possible to determine the limiting moment capacity for skirted foundations under very low vertical loads.

**Yun and Bransby** (2003) carried out a series of centrifuge model tests to investigate the response of skirted foundation on loose sand under combined vertical, horizontal, and flexural loading. The tests showed that the horizontal capacity of the skirted foundation increased to about 3-4 times that of plane foundation. They also suggested that the foundation failure mechanism changed from sliding to a rotational mode.

**Al-Aghbari and Mohamedzein** (2004) proposed modified bearing capacity equation for skirted strip foundations on dense sand. A series of tests on foundation models were carried out to study the factors that affect the bearing capacity of foundations with skirts. Several factors including foundation base friction, skirt depth, skirt side roughness, skirt stiffness and soil compressibility were studied and incorporated in a proposed equation. The results obtained from the proposed equation were compared with the results obtained from Terzaghi, Meyerhof, Hansen and Vesic bearing capacity equations for foundations without skirt. Comparison showed that the use of structural skirts can improve the bearing capacity by a factor of 1.5 to 3.9 depending on the geometrical and structural properties of the skirts and foundation, soil characteristics and interface conditions of the soil-skirt-foundation system.

**El Sawwaf and Nazer** (2005) presented results of laboratory model tests on the influence of soil confinement on the behavior of a model footing resting on granular soil. Confining cylinders with different heights and diameters were used to confine the sand. The ultimate bearing load of a circular footing supported on a three-dimensional confined sand bed was studied. Initially, the response of unconfined case was determined and then compared with that of confined soil. The results were then analyzed to study the effect of each parameter. The results indicated that the bearing capacity of circular footing can be appreciably increased by soil confinement. It was concluded that such reinforcement resists lateral displacement of soil underneath the footing leading to a significant improvement in the response of the footing. For small cell diameters, the cell-soil footing behaves as one unit (deep foundation), while this pattern of behavior was no longer observed with large cell diameters.

**Al-Aghbari and Mohamedzein** (2006) carried out tests on circular footing models with a structural skirt resting on sand. The results showed that the use of structural skirts improved the bearing capacity by a factor up to 3. At a working stress equal to 50% of the ultimate bearing capacity, the settlement of a surface footing can be reduced to just 11% of that for a footing without a structural skirt.

### **Soil Properties**

Karbala sand was used in the present study. Standard tests were performed to determine the physical properties of the sand. The tests were performed on sand

having two different densities; loose and medium sand. The details of these properties are listed in Table (1).

Laboratory characterization tests consisted of specific gravity, grain-size distribution, maximum and minimum dry density, and direct shear box tests. The grain size distribution of the sand used is shown in Figure (2). The soil is classified as (SP) according to the unified soil classification system.

### **Model square footing details**

Model square footing of 60 mm side was made of aluminum plate 10 mm thick, the base of the footing was covered with rough papers see Figure (3). The footing material has a modulus of elasticity of (65 GPa) (Al-Zayadi, 2010).

The wall was made of aluminum plate 650 mm in length, 310 mm in width and 10 mm in thickness, as shown in Figure (4). This wall is placed at different depths and different distances from the footing.

### **Model Setup Formulation**

All model tests were conducted using the setup, which consists of the following:

1. Steel container.
2. Steel base.
3. Steel loading frame.
4. Axial loading system.
5. Raining frame.
6. Impact hammer device.
7. Mechanical jack.
8. Load cell.
9. Digital weighting indicator.
10. Gear box.
11. AC Drive (speed regulator).
12. UPS.

### **Steel container and loading frame**

The steel container, manufactured for this study, has 0.75 m length, 0.75 m width, and 0.5 m height. It was made from five separated parts, one for the base and the others for the four sides. Each part of the container was made of 4 mm thick steel plate. At the internal sides of the container, a steel bar with 1 cm<sup>2</sup> cross sectional area was welded along three sides and the front side was kept free.

These shafts were welded each (100 mm) from bottom of the container. Steel plate (740×740) mm with 8 mm thickness was designed as a movable plate at any specific height instead of the original base plate; it was inserted inside the container and put on the welded bar and rested on it. This arrangement allows changing the height of soil bed that is being used.

A steel base was manufactured for this study to support the container and the loading frame weight. Steel loading frame was manufactured for this study to support the mechanical jack, axial loading system and gear box motor, as shown in Figure (5).

### **Axial loading system**

The axial loading system was manufactured for this study, the load is applied through a mechanical jack connected to a gear box motor and AC Drive (speed regulator), which in turn controls the speed of the gear box motor Figures (6). The maximum load that can be applied is about 2 tons. The loading rate is kept constant at 1 mm/min as recommended by Bowels (1978) for triaxial test.

**Raining frame**

The raining frame manufactured by Ali (2012), consists of two columns with changeable height. It was designed to achieve any desired elevation. The change of the frame height is done by holes with equidistance steps (15 cm). It is connected from top and bottom to the column with two joints to join 4 beams together. These beams are bolted at their ends. Two beams in the longitudinal direction have (U-section) and the other beams are used to support the U-section beams. Another beam was designed as a roller; it rests on the longitudinal beams to move along these beams. This (rolled-beam) is connected from the bottom with another beam, it is provided by screw and it can be moved horizontally along the beam; this beam was made to carry the cone that is used to pour the sand. The raining frame is illustrated in Figure (7).

This configuration of raining frame helps get a uniform density by controlling the height of fall. The rolled beam and the screw that is connected with the cone ensure that each particle drops from the same height to maintain uniform intensity.

A piece of mesh (diameter of the aperture is 10 mm) is put inside the cone to reduce the impact of the particles (Ali, 2012).

**Loading System**

The maximum load that can be applied through the mechanical jack, shown in Figure (8), is about 2 tons. A compression/tension load cell "SEWHA, Korea" model S-beam type: SS300 is used to measure the load. It is made of stainless steel – LS300, with a maximum capacity of 2 tons, locally calibrated, as shown in Figure (9). A digital weighing indicator is used for displaying the load amount "SEWHA, Korea" model SI 4010, with an input sensitivity of 50 gm as shown in Figure (10).

**Gear box**

Gear box is used to control the load. It is a motor with a high horsepower, it has capacity to apply high torques, as shown in Figure (11). It can control the speed of rotation through AC drive (regulator of speed). It is connected by a shaft to the mechanical jack. A device was connected directly to the gear box to control the speed of rotation by inserting the value of the required speed, as shown in Figure (12) (Mohammed, 2012).

**Sand Deposit Preparation**

The sand deposit was prepared using the sand raining technique. Five trials were performed to control the density of sand by raining technique. The sand was poured from different dropping heights (10, 20, 30, 40, and 50) cm to fulfill the same volume. The results show that the weight of sand required to fill the computed volume increases with increasing falling height, as a result, the sand density has a direct proportion with dropping height at specific boundaries. The effect of falling height on the controlled density is shown in Figure (13). After completing the final layer, the top surface is scraped and leveled by a sharp edge ruler to get as near as possible a flat surface.

The height of drop was chosen to be (20 and 50) cm which corresponds to a placing unit weight of (16.6 and 17.4) kN/m<sup>3</sup>, void ratio of (0.57 and 0.5) and relative density of (33 and 56) %, respectively. The properties of different states of sand used in the tests are listed in Table (2).

## Model Footings and Wall Preparations

### Model footings without wall

First, the bed of sand was prepared with controlled density as mentioned before. The final layer of the sand was leveled by a sharp edge ruler and then the footing was placed carefully in the center of the tank.

### Model square footing with a wall

First, the tank was filled with sand to the required level and the wall was installed at the specified distance and depth. The wall was then fixed well by screws linking the wall to the tank. After the wall has been installed in the tank, sand was deposited between the parts of the tank into the required level. The final layer of the sand was leveled by a sharp edge ruler and then the footing was placed in the tank as mentioned before.

### Testing Procedure

The procedure followed in testing the shallow footing model can be described in the following steps:

A vertical load was applied through a 2 ton capacity mechanical jack; a constant loading rate has been adopted in the entire testing program. The load was read from a digital weighing indicator connected to the load cell. The central displacement of the footing was read by one dial gage of 0.01 mm sensitivity. The load increments were continued until the total settlement exceeds about 10% and up to 20% of model footing width. The test is performed using strain controlled system, the settlement was read by one dial gage of 0.01 mm sensitivity.

The same procedure was followed for all footings at all relative densities (33, 56, and 75) %.

Some of during test photos are shown in Figure (14). The loading and measuring system assembly is shown in Figure (15).

For all model tests, the failure criterion adopted is that proposed by Terzaghi (1943) by which the failure load is defined as the load required to cause a settlement corresponding to 10% of the footing width.

### Theoretical Bearing Capacity

The values of the predicted bearing capacity are obtained from Terzaghi's equations:

$$q_{ult} = c N_c s_c + D_f \gamma N_q s_q + 0.5 B \gamma N_\gamma s_\gamma \quad \dots(1)$$

When:  $c = 0$  for granular soil, and  $D_f = 0$ , the equation becomes:

$$q_{ult} = 0.4 \gamma B N_\gamma \quad \dots(2)$$

for square footing

## Results of Tests

Forty-two model footing tests were performed to investigate the pressure-settlement relationships.

### Square footing tests on loose sand with $D_r = 33\%$

The bed of soil was prepared at a dry unit weight of  $16.6 \text{ kN/m}^3$  by assistance of raining technique. Fourteen model footing tests are carried out to find the observed pressure-settlement curves. Figures (16) to (19) represent the relationship between the pressure and settlement. Table (3) shows the predicted bearing capacity values

obtained from Terzaghi's Equation (2) compared with the values obtained from laboratory tests (observed).

From Figures (16) to (19), it is noticed that the shape of pressure-settlement curves indicates that punching shear failure is the governing mode of failure.

From Figures (16) and (17), it is clear that the presence of the wall near the footing affects the values of bearing capacity. The presence of wall along side of the footing resists the lateral displacement of the soil particles underneath the footing and confines the soil which in turn leads to a significant decrease in vertical settlement and hence improves the bearing capacity (El Sawwaf and Nazer, 2005). This increment in bearing capacity is significant when the wall is in contact with the footing ( $h/B = 0$ ), as well as at a distance of ( $h/B = 0.5$ ), and when the wall is at maximum depth ( $d/B = 2$ ), due to the increase in the soil confinement. The presence of the wall at a distance ( $h/B = 0.5$ ), affects the value of bearing capacity more than the effect at ( $h/B = 0$ ), because the increase in the mobilized vertical friction between the sand and the wall increases with the increase of the acting active earth pressure. These results are compatible with the findings of El Sawwaf and Nazer (2005). The density may not be equal in all regions. The density along the wall is less than the density in the center of the tank in case of the relative density (33 and 56) %.

From Figures (18) and (19), it is clear that further away of the wall from the footing, the bearing capacity effect approximately fades; due to the decrease in soil confinement. These results are compatible with the findings of El Sawwaf and Nazer (2005).

Figure (20) shows that the maximum effect of the wall on the value of bearing capacity is at ( $h/B = 0.5$ ) and decreases with increase of ( $h/B$ ), the wall effect on bearing capacity approximately fades at ( $h/B = 2$ ). These results are compatible with the results of Jawad (2006).

Figure (21) illustrates the relationship between the wall distance ( $h/B$ ) and bearing capacity ratio (BCR) which is defined as the ratio of the footing ultimate bearing capacity with the presence of wall to the footing ultimate bearing capacity in tests without wall. In Figure (21), the depth of the wall is kept constant ( $d/B=2$ ). It is noticed that the maximum effect of the wall on the value of bearing capacity ratio (BCR) is at ( $h/B = 0.5$ ) and decreases with the increase of ( $h/B$ ), the bearing capacity ratio effect approximately fades at ( $h/B = 2$ ). These results are compatible with the findings of Jawad (2006). From Figure (21), the values of bearing capacity ratio range from 1.06 to 1.43.

Figures (16) to (19), show the values of reduction in the vertical settlement (SRF) and settlement ratio ( $S_r$ ), the settlement was selected to be corresponding to the point of failure load ( $0.1B$ ) for footing without wall.

$$SRF = ((S_{\text{without wall}} - S_{\text{wall}}) / S_{\text{wall}}) * 100, \text{ and}$$

$$S_r = (S_{\text{wall}} / S_{\text{without wall}}) * 100.$$

The reduction in vertical settlement (SRF) ranges between (9 to 88) %, while the settlement ratio ( $S_r$ ) ranges between (53 to 92) %.

Al-Aghbari and Mohamedzein (2004) found similar results for skirted foundations. They stated that the use of structural skirts can improve the bearing capacity by a factor of 1.5 to 3.9 depending on the geometrical and structural properties of the skirts and foundation, soil characteristics and interface conditions of the soil-skirt-foundation system.

The improvement in bearing capacity can be explained as follows: when the footing is loaded, the wall confinement resists the lateral displacements of soil particles underneath the footing and confines the soil leading to a significant decrease in the vertical settlement and hence improving the bearing capacity.

The mobilized vertical frictions between the sand and the wall which increase with the increase of the acting active earth pressure until the point when the system starts to behave as one unit. The behavior is similar to that observed in deep foundations (piles and caissons) in which the bearing load increases due to the shear resistance of wall surface. This illustrates the increase of the bearing load with the increase of the distance and the depth of wall.

#### **Square footing tests on medium sand with $D_r = 56\%$**

These tests were performed at a dry unit weight of  $17.4 \text{ kN/m}^3$ . Fourteen model footing tests were performed to find the observed pressure-settlement relations. Figures (22) to (25) represent the relationship between the pressure and settlement. Table (3) shows the predicted bearing capacity values obtained from Terzaghi's equation (2) compared with the values obtained from laboratory tests (observed).

From Figures (22) to (25), it is noticed that the shape of pressure-settlement curves indicates that local shear failure is the governing mode of failure.

Figures (22) to (25) are pursuing the same behavior of the previous tests (square on loose sand at relative density 33%). The reduction in vertical settlement (SRF) ranges between (9 to 150) %, while the settlement ratio ( $S_r$ ) ranges between (40 to 92) %. Figures (26) and (27) show that the optimum value of bearing capacity is at ( $h/B = 0.5$ ) and decreases with increase of ( $h/B$ ), after that, the effect of wall on bearing capacity approximately fades at ( $h/B = 2$ ). These results are compatible with the results of El sawwaf and Nazer (2005). The values of bearing capacity ratio range from 1.04 to 1.56.

#### **Effect of Wall Depth on the Bearing Capacity Ratio for Different Wall Distances from the Footing**

##### **Square footing resting on sand with different densities**

The relationship between the BCR and  $d/B$  is shown in Figures (28) and (29), for different distances ( $h/B$ ) from the footing. It can be seen that footing with wall improved the performance of the footing by increasing the bearing capacity and reducing the settlement of the system.

Figures (28) and (29) clearly show that the footing performance improves much with the increase of wall depth. The degree of improvement varies depending on the wall depth and the location of the footing from the wall. The presence of the wall along side of the footing resists the lateral displacement of the soil particles underneath the footing and confines the soil which in turn leads to a significant decrease in vertical settlement and hence improves the bearing capacity. The mobilized lateral resistance along the wall increases with increase of wall depth. The effectiveness of this confinement is dependent on some factors. These factors include the location of the footing from the wall, the wall depth and interaction of the wall with the failure plane. These results are compatible with those obtained by Azzam and Farouk (2010).

Figures (28) and (29) illustrate that there is no benefit behind increasing the penetration depth of the wall beyond a limit value of ( $d/B = 2$ ). A considerable decrease in BCR is noticed when the wall depth is less than ( $1.5 B$ ). This can be due

to the fact that when ( $d/B < 1.5$ ), the wall length provides only partial confinement to the soil. These results agree with the findings of Azzam and Farouk (2010).

### **Effect of Wall Distance on the Bearing Capacity Ratio for Different Depths below the Footing**

The relationship between the BCR and  $h/B$  is shown in Figures (30) and (31) for different depths of the wall ( $d/B$ ). It can be seen that the presence of a wall improves the performance of the footing by increasing the bearing capacity and reducing the settlement of the system. Figures (30) and (31) show that further away of the wall from the footing, the effect of wall on bearing capacity effect approximately fades, due to the decrease in soil confinement. These results agree with the findings of El Sawwaf and Nazer (2005).

Figures (30) and (31) illustrate that no effect is gained when increasing the distance of the wall from the footing beyond a limit value of ( $h/B = 1$ ) for all depths of the wall, experiments for ( $h/B = 1.5$  and  $2$ ) are carried out for ( $d/B = 2$ ) and not carried out for all depths of the wall. These results agree with the findings of El Sawwaf and Nazer (2005) and Jawad (2006).

### **CONCLUSIONS**

1-The presence of the wall near a footing affects remarkably the bearing capacity, leading to improvement in the bearing capacity with different percentages according to the distance of the wall from the edge of footing and depth of wall, due to the increase in the soil confinement underneath the footing. In loose sand, the largest improvement in bearing capacity for square footing bounded by walls reaches (43) %, at ( $h/B = 0.5$ ) and ( $d/B = 2$ ). In medium sand, the largest improvement in bearing capacity for square footing bounded by walls reaches (56) %, at ( $h/B = 0.5$ ) and ( $d/B = 2$ ).

2-The presence of the wall mitigates the vertical settlement, the largest reduction in the vertical settlement (SRF) ranges from (9 to 150) % in all tests depending on the wall depth and its distance from the footing.

3-In loose and medium sand, the maximum effect of the wall on the value of bearing capacity is when the distance between the wall and the footing edge; ( $h/B$ ) is 0.5 of footings.

4-The bearing capacity increases with the depth of the wall, the maximum effect of the wall on the bearing capacity is when the value of the depth of the wall to width of the footing ratio ( $d/B$ ) is between (1.5-2.0), for footing on sand of different densities.

5-When the existence of the wall is at a large distance from footing, the bearing capacity effect approximately fades at ( $h/B=2$ ) due to the decrease in soil confinement.

### **REFERENCES**

- [1]Al-Aghbari, M.Y. and Mohamedzein, Y.E. (2004): "Bearing Capacity of Strip Foundations with Structural Skirts", Journal of Geotechnical and Geological Engineering, Springer publishing, Vol. 22, No.1, pp. 43-57.
- [2]Al-Aghbari, M.Y. and Mohamedzein, Y.E. (2006): "Improving the Performance of Circular Foundations Using Structural Skirts", Journal of Ground Improvement, ICE, UK, Vol. 10, No.3, pp. 125-132.
- [3]Ali, A.M. (2012): "Effect of Scaling Factor on Pile Model Test Results", M.Sc. Thesis, Building and Construction Engineering Department, University of Technology, Iraq.

- [4]Al-Zayadi, A. A. (2010): "Three Dimensional Analysis of Piled Raft Foundation", PhD. thesis, University of Baghdad, Iraq.
- [5]ASTM D3080-1998, "Standard Test Method for Direct Shear Test of Soils under Consolidated Drained Conditions", American Society for Testing and Materials.
- [6]ASTM D4253-2000, "Standard Test Method for Maximum Index Density and Unit Weight of Soils Using a Vibratory Table", American Society for Testing and Materials.
- [7]ASTM D4254-2000, "Standard Test Method for Minimum Index Density and Unit Weight of Soils and Calculation of Relative Density", American Society for Testing and Materials.
- [8]ASTM D422-2001, "Standard Test Method for Particle Size-Analysis of Soils", American Society for Testing and Materials.
- [9]ASTM D854-2005, "Standard Test Method for Specific Gravity of Soil Solids by Water Pycnometer", American Society for Testing and Materials.
- [10]Azzam, W.R. and Farouk, A. (2010): "Experimental and Numerical Studies of Sand Slopes Loaded with Skirted Strip Footing", *Electronic Journal of Geotechnical Engineering EJGE*, Vol. 15, pp. 795-812.
- [11]Bowels, J.E. (1978): "Engineering Properties of Soils and Their Measurement", Second Edition, McGraw-Hill International Book Company, Tokyo, Japan.
- [12]Byrne, B.W., Villalobos, F., Houlsby, G.T. and Martin C.M. (2002): "Laboratory Testing of Shallow Skirted Foundations in Sand", Department of Engineering Science, The University of Oxford, Title, Thomas Telford, London.
- [13]El Sawwaf, M. and Nazer, A. (2005): "Behavior of Circular Footings Resting on Confined Granular Soil", *Journal of Geotechnical and Geoenvironmental Engineering*, ASCE, Vol. 131, No.3, pp. 359-366.
- [14]Jawad, I.T. (2006): "Effect of Confinement on Bearing Capacity and Settlement of Spread Foundation Using ANSYS Program", M.Sc. Thesis, Building and Construction Engineering Department, University of Technology, Iraq.
- [15]Mohammed, H. A., (2012), "Experimental and Statistical Study on the Behavior of Bounded Foundations on Sandy Soil", M.Sc. thesis, Building and Construction Engineering Department, University of Technology, Baghdad, Iraq.
- [16]Rao, B.G. and Narhari, D.R. (1979): "Skirted Soil Plug Foundation", Proc. 6th Asian Regional Conference on Soils, Singapore, pp. 319-322 (Cited by Saleh et al., 2008).
- [17]Rao, B. G. and Ranjan, G. (1985): "Settlement Analysis of Skirted Granular Piles", *Journal of Geotechnical Engineering Division*, ASCE, Vol. 111, No.11, pp.1264-1283.
- [18]Saleh, N.M., Alsaied, A.E. and Elleboudy, A.M. (2008): "Performance of Skirted Strip Footing Subjected to Eccentric Inclined Load", *Electronic Journal of Geotechnical Engineering EJGE*, Vol. 13, pp. 1-33.
- [19]Yun, G.J. and Bransby, M.F. (2003): "Centrifuge Modeling of the Horizontal Capacity of Skirted Foundations on Drained Loose Sand", Proc. International Conference on Foundations, Dundee, Scotland, pp. 1-10.

**Table (1) Physical properties of the sand used in the present tests.**

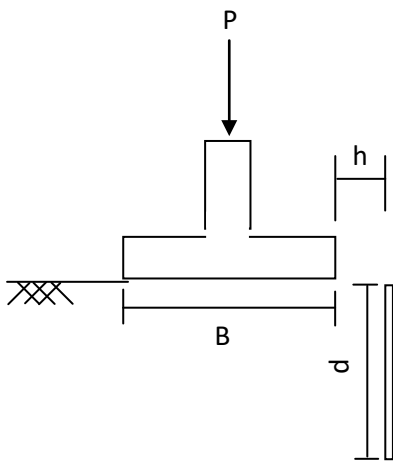
No.	Index property	Value	Specification
A	Grain size analysis		ASTM D 422-2001
1	D <sub>10</sub> (mm)	0.16	
2	D <sub>30</sub> (mm)	0.36	
3	D <sub>60</sub> (mm)	0.57	
4	Coefficient of uniformity (C <sub>u</sub> )	3.56	
5	Coefficient of curvature (C <sub>c</sub> )	1.42	
6	Soil classification (USCS)	SP	
7	Specific gravity (G <sub>s</sub> )	2.66	ASTM D 854-2005
B	Dry unit weights		
8	Maximum dry unit weight (kN/m <sup>3</sup> )	19.1	ASTM D 4253-2000
9	Minimum dry unit weight (kN/m <sup>3</sup> )	15.6	ASTM D 4254-2000
C	Void ratios		
10	Maximum void ratio	0.67	
11	Minimum void ratio	0.36	

**Table (2) Properties of different states of sand used in the tests.**

State of sand	Dry unit weight (γ <sub>d</sub> ) (kN/m <sup>3</sup> )	Void ratio	Angle of friction (φ)*	Relative density (Dr %)
Loose	16.6	0.57	34°	33
Medium	17.4	0.5	37°	56

\*Note: Direct shear test was performed according to the ASTM D 3080-98.

Table (3) Summary of the predicted and observed ultimate model square footing bearing capacities.

Test No.	Distance of the wall (h/B)	Depth of the wall (d/B)	Predicted bearing capacity from Terzaghi's equation (kN/m <sup>2</sup> )		Observed bearing capacity (kN/m <sup>2</sup> )	
			$\phi = 34^\circ$	$\phi = 37^\circ$	$\phi = 34^\circ$	$\phi = 37^\circ$
1	-	-	15	27.4	29.4	34.2
2	0	0.5			30.9	41.6
3	0	1			34.7	45.9
4	0	1.5			36.4	49.3
5	0	2			39.1	50.5
6	0.5	0.5			31.9	42.5
7	0.5	1			35.8	48.1
8	0.5	1.5			41.0	51
9	0.5	2			42.0	53.3
10	1	0.5			30.9	41.6
11	1	1			34.7	43.6
12	1	1.5			35.7	44.7
13	1	2			36.4	46.0
14	1.5	2			33.4	40.7
15	2	2			31.1	35.7

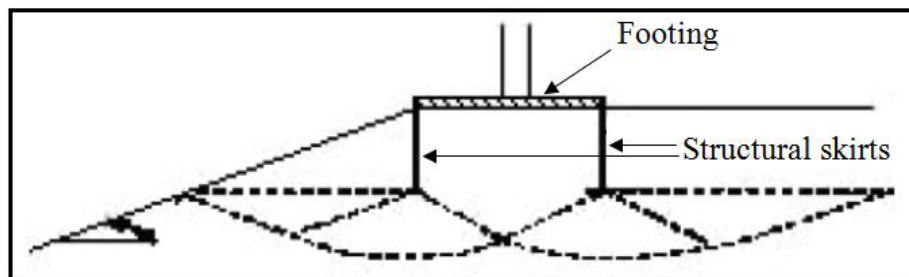


Figure (1) Bearing capacity failure mechanism in strip footings with structural skirt subjected to vertical central load (after Azzam and Farouk, 2010).

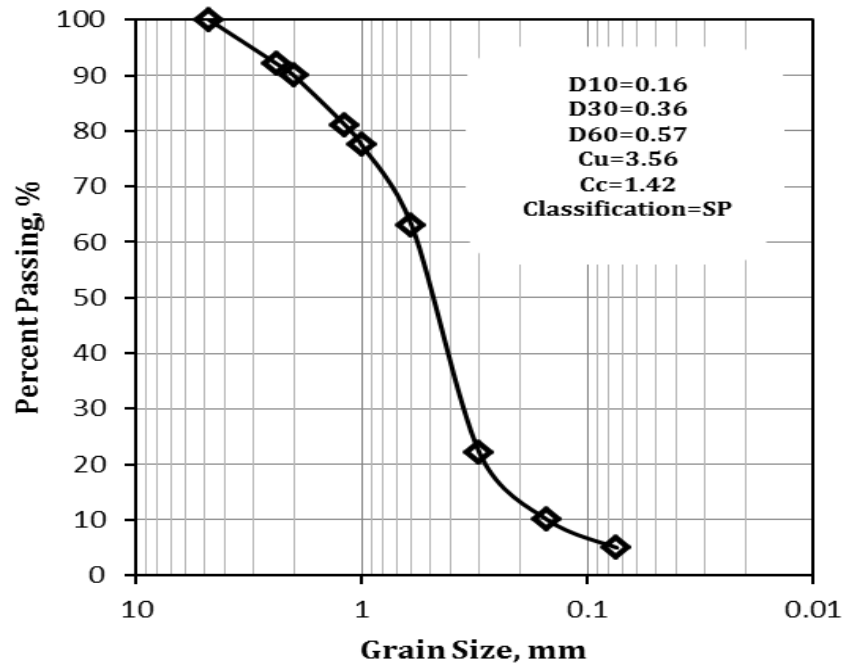
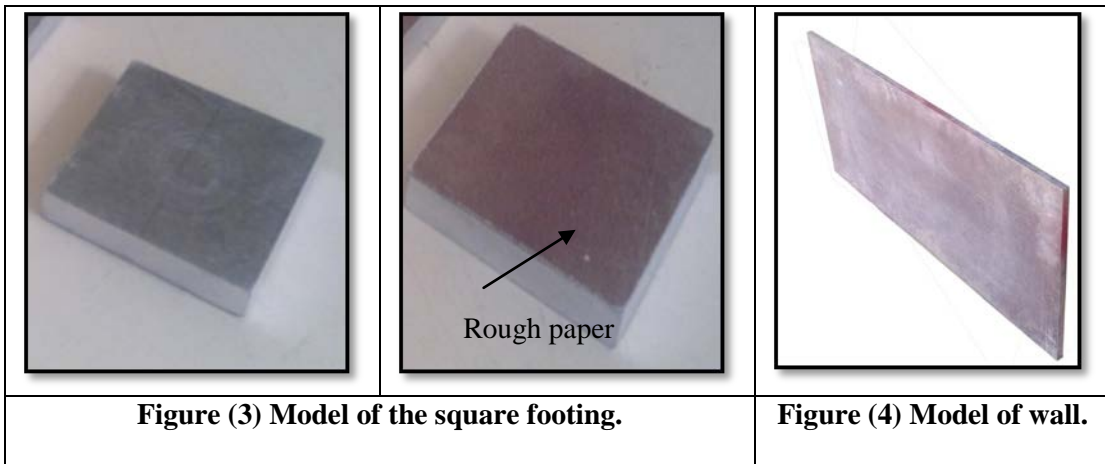


Figure (2) Grain size distribution of the sand.





**Figure (5) Steel loading frame.**



**Figure (6) The axial loading system.**



**Figure (7) Raining frame used for controlling density.**



Figure (8) Mechanical jack.



Figure (9) Load cell.



Figure (10) Digital weighing indicator.



Figure (11) Gear box.



Figure (12) AC drive (Regulator of speed).

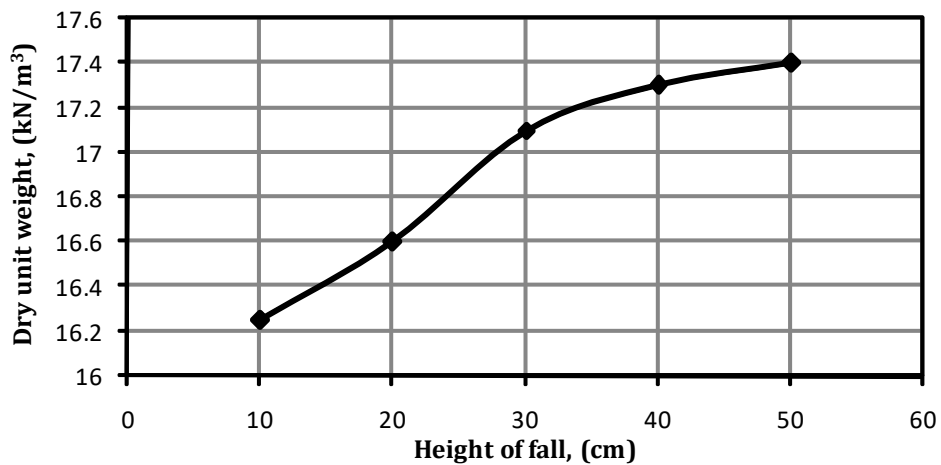


Figure (13) Relationship between dry unit weight of the sand used and height of fall.



a. ( $h/B = 0$ ).

b. ( $h/B = 0.5$ ).

c. ( $h/B = 1$ ).

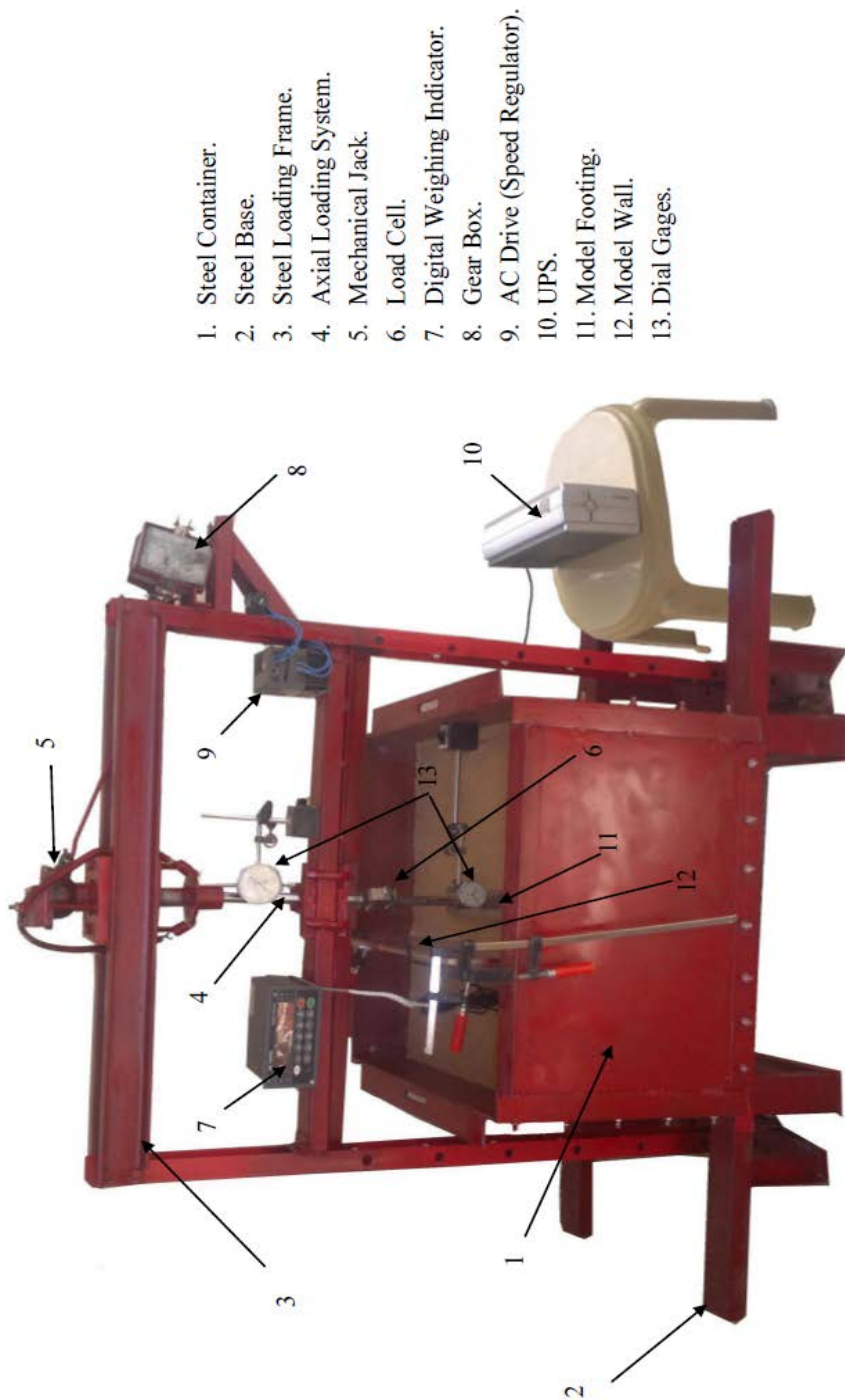


d. ( $h/B = 1.5$ ).



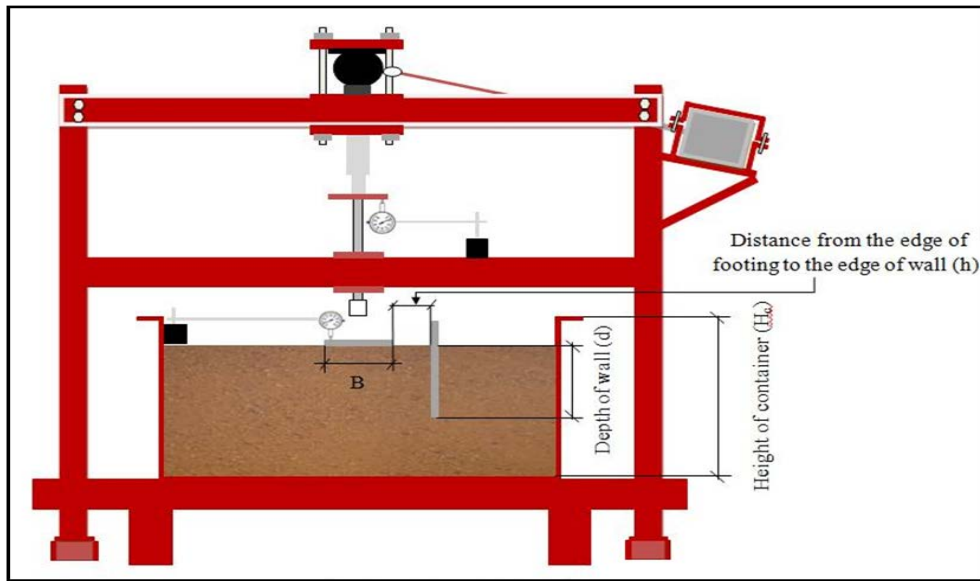
e. ( $h/B = 2$ ).

**Figure (14) During test photographs.**



1. Steel Container.
2. Steel Base.
3. Steel Loading Frame.
4. Axial Loading System.
5. Mechanical Jack.
6. Load Cell.
7. Digital Weighing Indicator.
8. Gear Box.
9. AC Drive (Speed Regulator).
10. UPS.
11. Model Footing.
12. Model Wall.
13. Dial Gages.

a. Isometric view of the apparatus.  
Figures 15 Testing system assembly.



b. Front view of the apparatus, Figure (15) (continued).

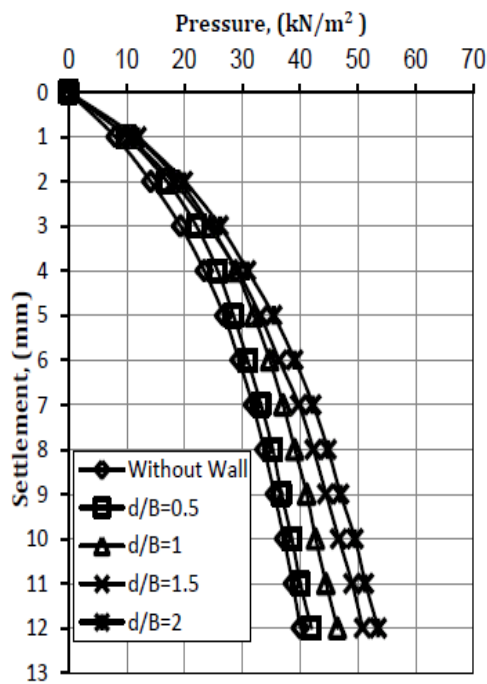


Figure (16) Pressure-settlement relationships for footing with ( $h/B = 0$ ) resting on loose sand.

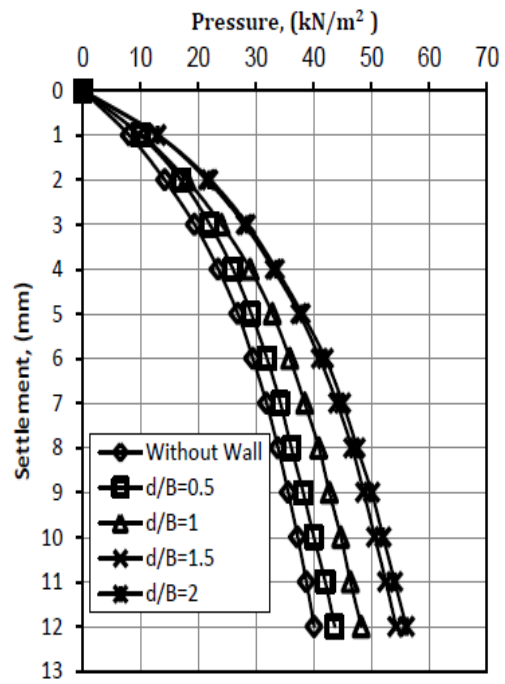


Figure (17) Pressure-settlement relationships for footing with ( $h/B = 0.5$ ) resting on loose sand.

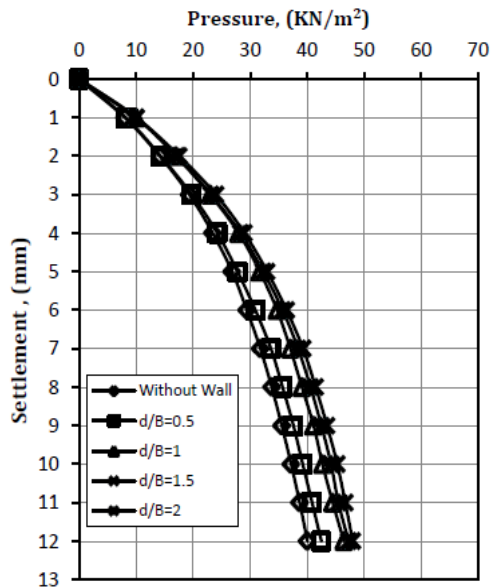


Figure (18) Pressure-settlement relationships for footing with ( $h/B = 1$ ) resting on loose sand.

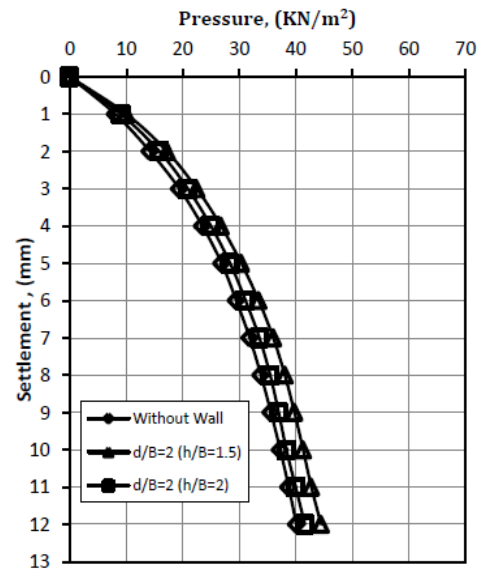


Figure (19) Pressure-settlement relationships for footing with ( $h/B = 1.5$ ) and ( $h/B = 2$ ) resting on loose sand.

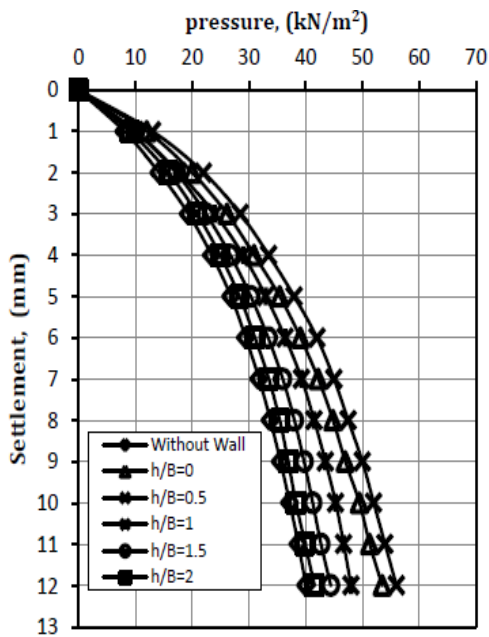


Figure (20) Pressure-settlement relationships for footing with ( $d/B = 2$ ) resting on loose sand.

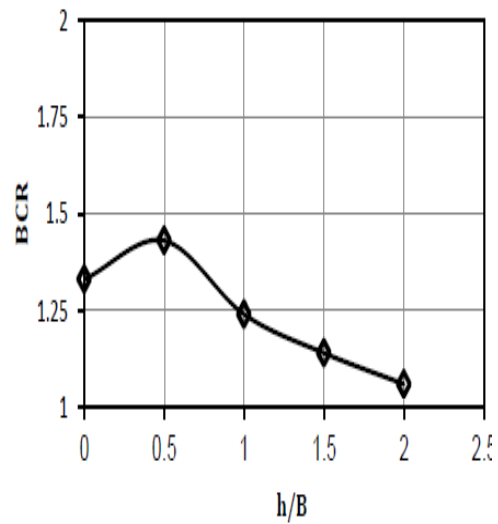


Figure (21) Bearing capacity ratio of square footing bounded by a wall with  $d/B = 2$  at different distances, resting on loose sand with  $Dr = 33\%$ .

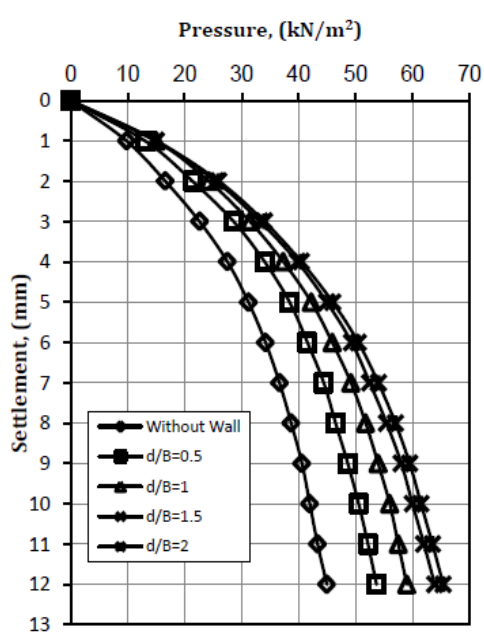


Figure (22) Pressure-settlement relationships for footing with ( $h/B = 0$ ) resting on medium sand.

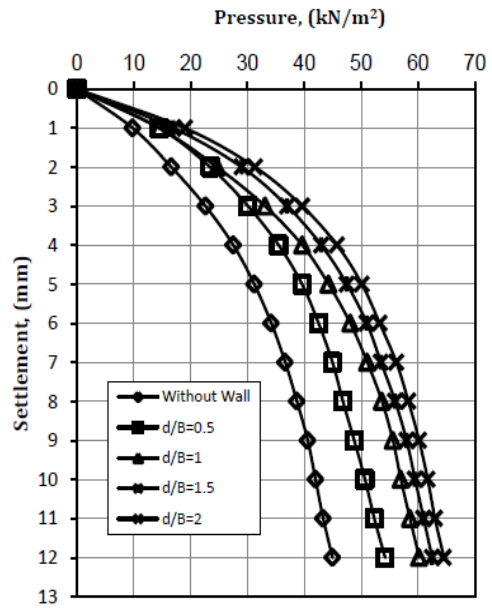


Figure (23) Pressure-settlement relationships for footing with ( $h/B = 0.5$ ) resting on medium sand.

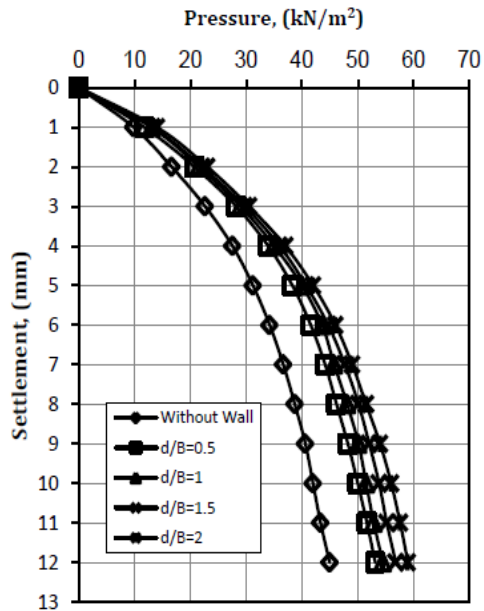


Figure (24) Pressure-settlement relationships for footing with ( $h/B = 1$ ) resting on medium sand.

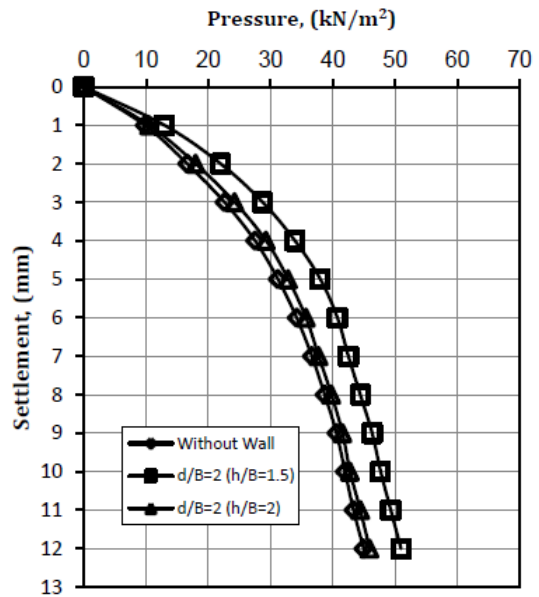


Figure (25) Pressure-settlement relationships for footing with ( $h/B = 1.5$ ) and ( $h/B = 2$ ) resting on medium sand.

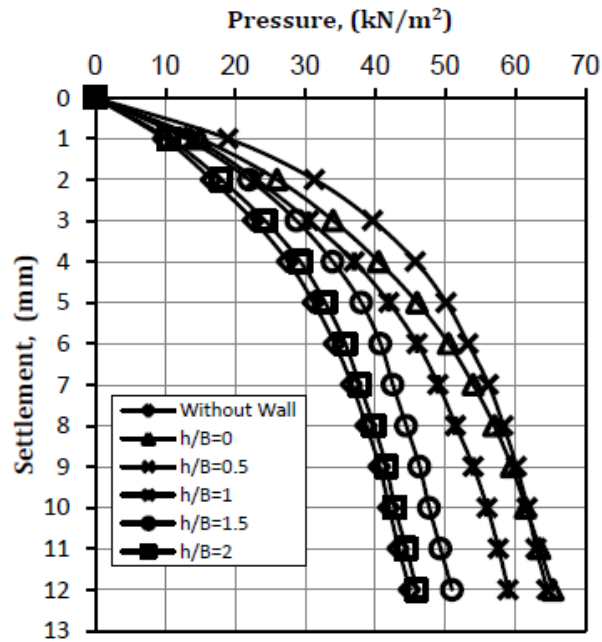


Figure (26) Pressure-settlement relationships for footing with ( $d/B = 2$ ) resting on medium sand.

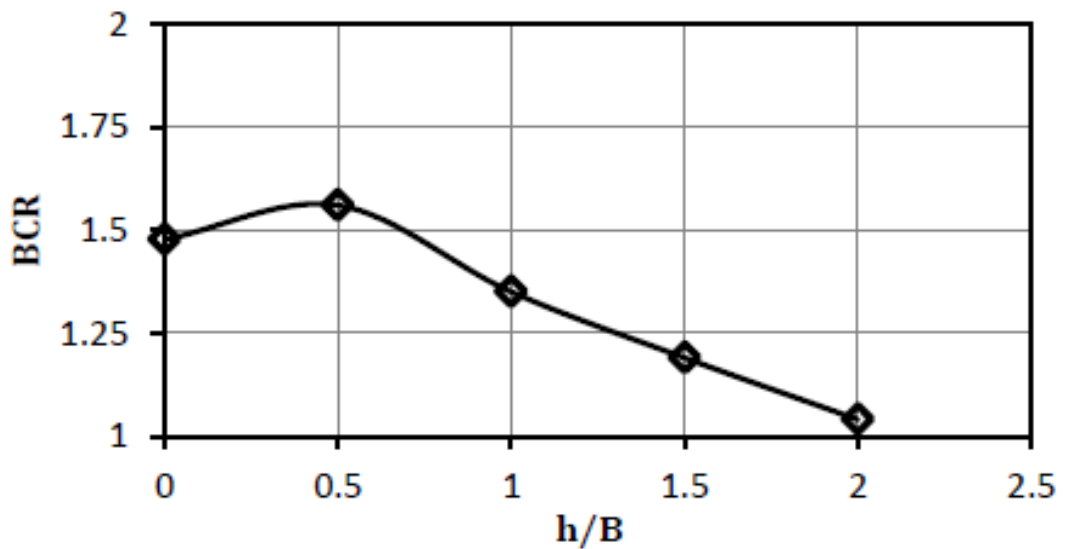


Figure (27) Bearing capacity ratio of square footing bounded by a wall with  $d/B = 2$  at different distances, resting on medium sand with  $D_r = 56\%$ .

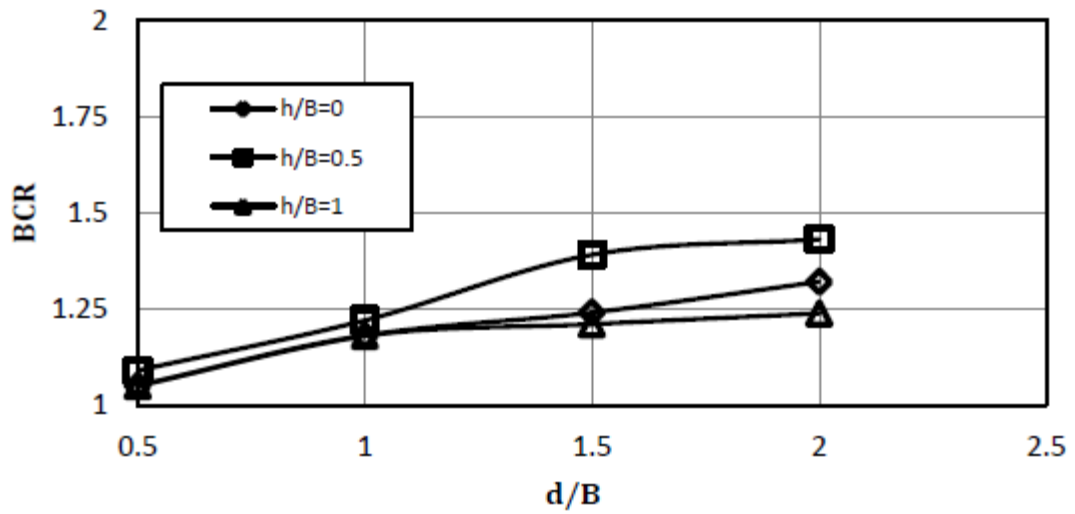


Figure (28) Effect of wall depth at different distances on bearing capacity ratio of footing resting on loose sand with  $D_r = 33\%$ .

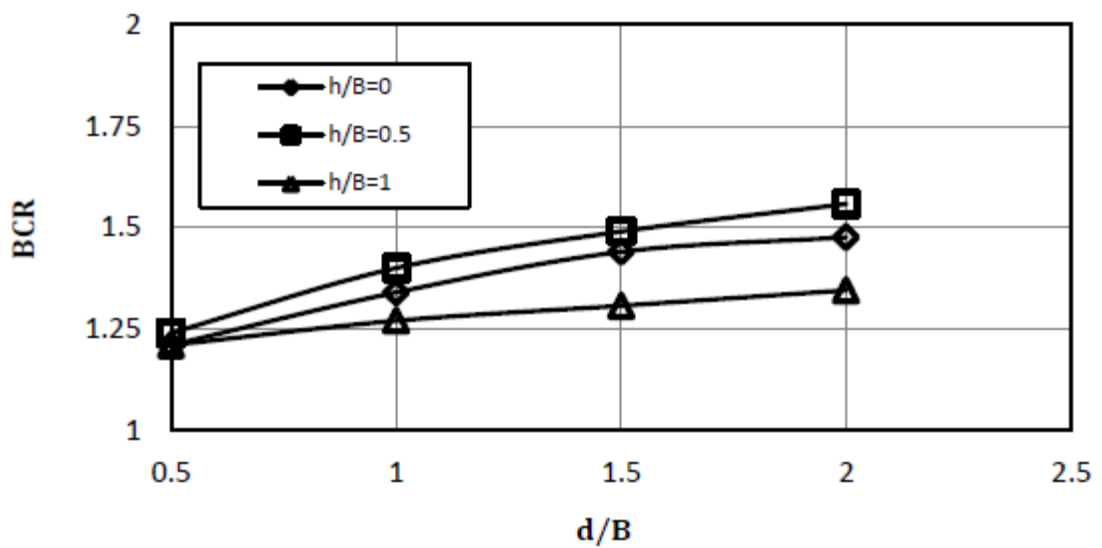


Figure (29) Effect of wall depth at different distances on bearing capacity ratio of footing resting on medium sand with  $D_r = 56\%$ .

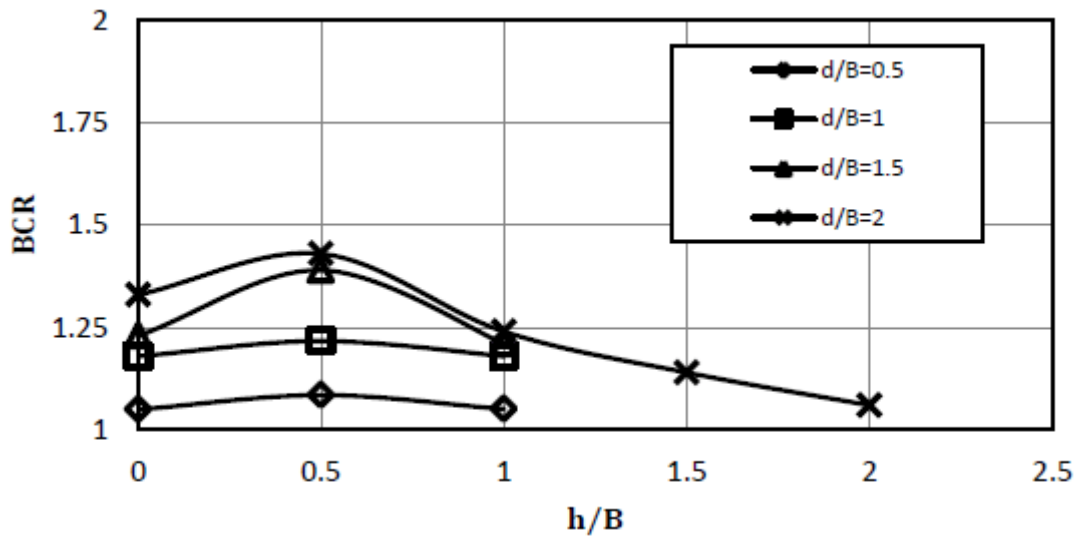


Figure (30) Effect of wall distances at different depths on bearing capacity ratio of footing resting on loose sand with  $D_r = 33\%$ .

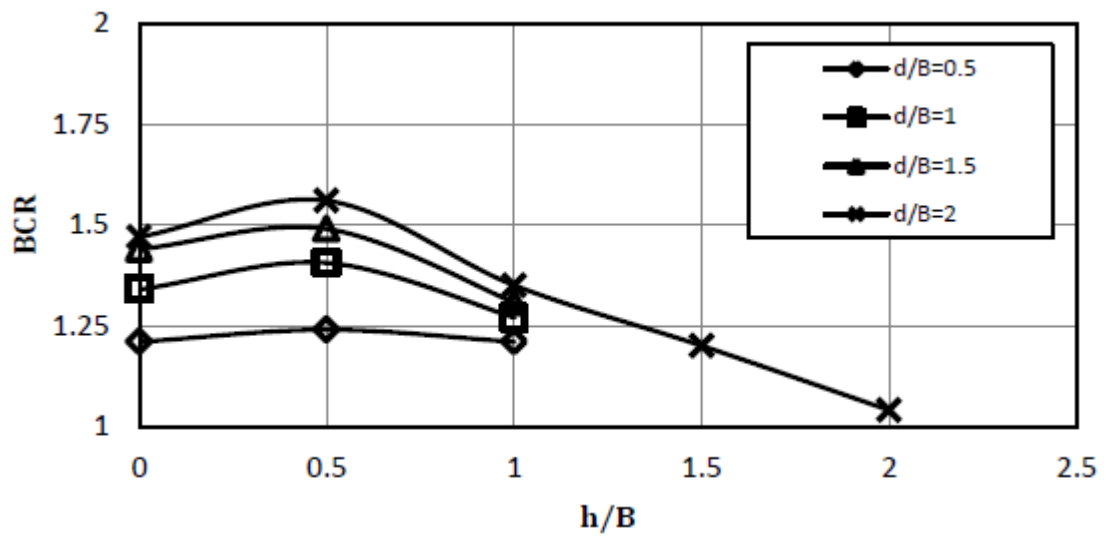


Figure (31) Effect of wall distances at different depths on bearing capacity ratio of footing resting on medium sand with  $D_r = 56\%$ .